Journal of Physics: Conference Series **525** (2014) 012021 doi:10.1088/1742-6596/525/1/012021

Benchmarking of a novel contactless characterisation method for micro thermoelectric modules (μTEMs)

S. Hickey[1], J. Punch[1], N. Jeffers[2]

[1] CTVR, Stokes Institute, University of Limerick, Limerick, Ireland
[2] Thermal Management Research Group, Bell Labs, Alcatel-Lucent Ireland, Blanchardstown, Dublin 15, Ireland

E-mail: seamus.hickey@ul.ie

Abstract. Significant challenges exist in the thermal control of Photonics Integrated Circuits (PICs) for use in optical communications. Increasing component density coupled with greater functionality is leading to higher device-level heat fluxes, stretching the capabilities of conventional cooling methods using thermoelectric modules (TEMs). A tailored thermal control solution incorporating micro thermoelectric modules (μTEMs) to individually address hotspots within PICs could provide an energy efficient alternative to existing control methods. Performance characterisation is required to establish the suitability of commercially-available μTEMs for the operating conditions in current and next generation PICs. The objective of this paper is to outline a novel method for the characterisation of thermoelectric modules (TEMs), which utilises infra-red (IR) heat transfer and temperature measurement to obviate the need for mechanical stress on the upper surface of low compression tolerance (~0.5N) μTEMs. The method is benchmarked using a commercially-available macro scale TEM, comparing experimental data to the manufacturer's performance data sheet.

1. Introduction

Photonics Integrated Circuits (PICs) increasingly feature in today's optical communication systems, in order to realise devices with greater spectral efficiency and reduced power losses. PICs can represent a stringent packaging challenge, however, particularly in terms of their requirements for thermal control. Devices such as laser arrays can feature tight temperature limits (±0.1K), low operating temperatures (as low as 45°C), moderate heat loads (~1W) but very high heat fluxes (over 10^2 W/cm^2). Addressing the areas of high heat flux directly using micro Thermoelectric Modules (μTEMs) reduces the need for heat spreading and reduces the energy required to maintain temperature control in PICs. Characterising commercially-available μTEMs is essential to determine their suitability for PIC applications. Literature has documented the characterisation of macro scale TEMs extensively [1-8] but has not yet reported the precise characterisation of micro scale devices. TEM characterisation consists of two distinct approaches in published works. The first is the characterisation of thermoelectric parameters [1-5] such as Seebeck coefficient (α), module conductivity (K_M) and module electrical resistance (R), leading to the calculation of the thermoelectric figure of merit (Z). This approach is concerned with the fundamental thermoelectric material properties and their efficiency in TEM operation. The second approach is considered a more top level view of TEM application and is

concerned with measuring the performance characteristics [6-9] for TEMs which can be used determine the suitability of a device for particular operating conditions. The relevant performance characteristics are the temperature difference across the device, (T_h - T_c = ΔT), and heat pumped from the cold side of the module, (Q_c), both of which are a function of the current (I) through the TEM. It is the latter approach which is pursued in this study to determine the suitability of µTEMs for use in PIC applications. Problems exist however, preventing the use of conventional TEM characterisation methods, chief among them being the low compressive load bearing capacity of µTEMs (~0.5N) compared to conventional TEMs (~100N). Most characterisation methods [2-9] rely on compressing the TEM between a heat source and sink in order to measure the characteristics of the device. Methods which obviate the need for contact with the upper surface of the µTEMs avoid potential damage to the devices while providing relevant performance data. To this end, an experimental setup is developed in this paper which utilizes an infra-red (IR) heating element to deliver heat to the µTEMs and a calorimeter to quantify the heat pumped through them. It is proposed that this novel method of characterisation be proven on macro scale TEMs and compared to existing standards as part of an overall body of work investigating the suitability of µTEMs for use in photonics packaging.

The objective of this paper is to accurately characterise the thermal performance of a TEM using contactless heat application in the form of an IR source. The method is subjected to an uncertainty analysis and is benchmarked using quoted performance data from the manufacturer. The outcome is the demonstration of a novel characterisation method for TEMs which does not require thermal contact with the device.

2. Experimentation

An experimental characterisation setup, illustrated in figure 1, was devised to deliver heat to the upper surface of a test TEM in a contactless fashion via an IR heat source, while measuring the heat pumped through the device (Q_c) using a calorimeter and temperature difference across it (ΔT) with an IR temperature sensor and thermistors. The setup was placed in a vacuum to eliminate condensation on the upper TEM surface at low temperatures and to minimise losses due to convection. This section details the components of the experimental apparatus assembly and test procedure. An analysis of experimental measurement and uncertainty is discussed in section 3, data reduction.

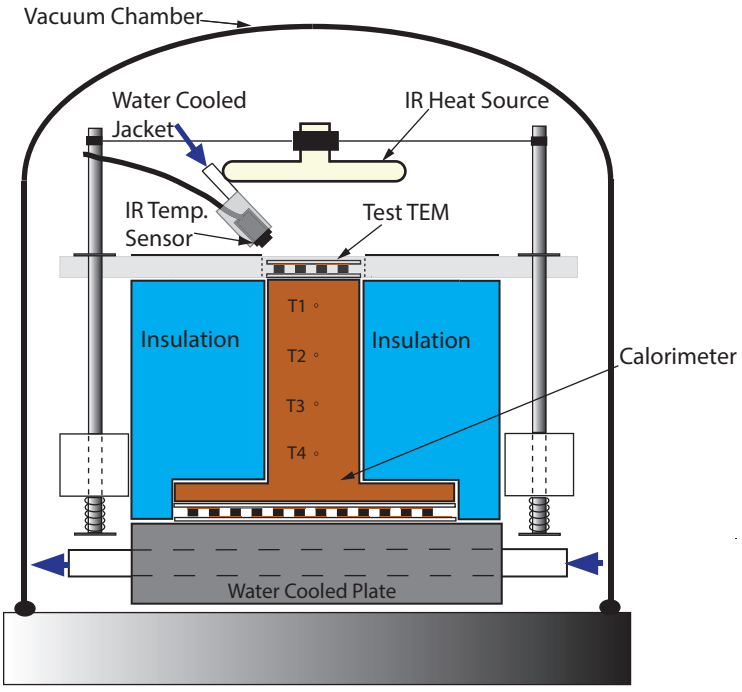

Figure 1. Schematic of contactless characterisation apparatus

2.1 Apparatus

A calorimeter was machined to the dimensions of 15 x 15 x 40mm with a base of 30 x 30 x 5mm using oxygen free copper (395 W/m K). Four 0.82mm holes were drilled 3mm deep at 5, 15, 25 and 35mm from the surface in which were embedded four 0.8mm diameter, 1.2mm long, 5kΩ Epcos B57540G502F thermistors in order to measure the temperature gradient along the length of the calorimeter. Temperature measurements from the embedded thermistors were recorded using Labview software. From this temperature gradient, the heat transfer from (Q_h), and temperature of (T_h), the lower surface of the TEM, referred to as the hot side, was determined. The upper face of the copper calorimeter was polished to a mirror finish ensuring that planarity was maintained. Polyurethane foam insulation (0.035 W/m K) was placed around the calorimeter to minimise thermal losses. The copper calorimeter was placed on a secondary TEM, European Thermodynamics model number ET-241-14-15, in order to hold T_h at 25°C (298K) via PID control using Labview software. This was then mounted on a water cooled aluminium block with water circulated at 10°C by a Lauda E100 water bath. All interfacing surfaces were coated with a thin layer of Electrolube HTSP heat transfer compound to reduce thermal resistance at the interfaces.

Benchmarking tests were carried out on a Multicomp MCPF-031-10-25 single stage TEM of dimensions 15 x 15 x 4.8mm. The upper surface of the TEM, referred to as the cold side, was coated with a 20μm layer of matte black paint to increase the IR absorptivity of the ceramic surface. The test TEM was fixed in place by a spring clamping mechanism. Polycarbonate sheet, 5mm thick, was machined to hold the TEM at each of the four corners, leaving a minimal area of the TEM surface in contact with the clamp and almost the entire face of the TEM exposed. The clamp was fixed to two spring loaded stainless steel rods which applied the downward force. Two steel springs, each 2.5kN/m stiffness, applied a minimum of 50N downwards force. This imposed a pressure of 222kPa over the area of the test TEM to minimise interfacial thermal resistance.

The contactless heat source for the apparatus was a 125W Ceramicx IR quarter flat ceramic heater which was fixed 45mm above the test TEM using steel guide rods and heat resistant rubber rings in order to adjust its height. The heater was connected to a variable power source in order to adjust the heat supplied to the test TEM. Low emissivity (< 0.1) aluminium foil was used where appropriate to reduce stray radiation heat transfer from the heater to the calorimeter and electrical wires within the bell jar. Temperature on the cold side of the module (T_c) was measured by a Raytek MI3 miniature IR sensor with close focus sensing head targeting a spot size of 1mm^2 on the centre of the TEM surface. The temperature reading was processed and recorded by Raytek's Data Temp Multidrop software. The sensor was positioned using a specially designed mounting bracket machined in polycarbonate, which was angled to the precise angle of view and distance from the test surface to produce a 1mm^2 spot size for temperature measurement. Due to the proximity of the miniature IR sensor to the heater, steps were taken to prevent the sensing head from heating up excessively. To this end, a water-cooled aluminium jacket was machined and placed around the sensing head, with water circulated through it by the water bath at a temperature of 10°C.

Constant current was conveyed to the TEM under test using a TTi QL355TP power supply, with measurements of voltage and current taken using certified calibrated Fluke 45 and Fluke 37 multimeters respectively. Voltage measurements were taken across the test device as close as possible to the positive and negative terminals to minimise uncertainty attributed to resistance in the electrical wires. The experimental setup was placed on an aluminium baseplate 380mm in diameter and covered by a glass bell jar 320mm in diameter and 360mm in height. This was evacuated to an absolute vacuum of approximately 400Pa, the lowest achievable vacuum for this setup using a PVR PHV-5 vacuum pump. At this vacuum, moisture is removed from the air preventing condensation build up on the upper TEM surface at low temperatures. The purpose of this was to prevent moisture in the air condensing on the cold side surface of the TEM at low temperatures and to reduce convective losses. Vacuum rated water fittings were used to supply the water cooled plate and IR sensor cooling jacket with water from the water bath. Electrical power supply wires and sensing wires were connected across the aluminium base plate by vacuum rated electrical fittings with connectors on both sides.

Vacuum losses were reduced by using a rubber sealing ring around the bottom of the bell jar and Dow Corning high vacuum silicone grease.

Having described the experimental apparatus in detail, the experimental procedure is outlined in the following subsection.

2.2 Test procedure

The objective of the test procedure was to benchmark the apparatus using a commercially available TEM. According to the data sheet provided by the manufacturer, the test conditions for the quoted data were for T_h maintained at 25°C over a current range of *0.4A – 2.0A* in steps of *0.4A*, using the AC four terminal method [1]. In order to measure the thermal performance characteristics of the TEM using the contactless apparatus detailed above, the following test procedure was developed to be highly repeatable while minimising areas of variance and possible uncertainty:

- The water bath was switched on one hour in advance of each test to allow the water to cool from room temperature to the test condition of 10°C and to enable the water cooled plate and IR sensor jacket to reach steady state.
- The test TEM was fitted in place on the upper surface of the calorimeter with a thin layer of heat transfer compound on the contact surface. The spring loaded clamping mechanism was then applied to hold it in place.
- The miniature IR sensor was positioned using its custom mounting bracket. Positional repeatability was ensured using physical stops to place the bracket.
- The IR heater was then put in place above the test TEM surface. Initially the heater remained off for the case of minimum heat flow, 0W.
- The bell jar was then placed over the apparatus and sealed to the vacuum plate. The vacuum release valve was then closed and the vacuum pump was switched on.
- The test TEM was powered with a constant current set to 0.4A. The system was allowed to reach steady state with T_h maintained at 25°C; on average this took between 15 to 20 minutes.
- Electrical measurements of TEM voltage and current were then taken.
- Cold side temperature and the temperature gradient along the calorimeter were recorded and averaged over a five minute interval.
- Test TEM current was then raised in steps of 0.4A as far as 2A, allowing each step to reach steady state. Electrical and temperature measurements were again recorded for each current step.
- Upon collecting a full set of data for the current range, the heater power was then increased in steps of 20W up to a maximum of 120W. Increasing the heater power also increased the time required to reach steady state thermally, when compared to adjusting TEM current, requiring approximately 45 minutes.
- The procedure was repeated for each current setting until a complete set of data was attained for all heater power settings.

The experimental measurements were ultimately used to compare the TEM performance characteristics provided by the manufacturer and those obtained using the contactless apparatus. In order to use the data collected, a formal data reduction and uncertainty analysis was required, and this is detailed below in section 3.

3. Data reduction

Presented in this section are all the calculated variables derived from experimental data with each of their related primary variables. Their relevance to the overall TEM characterisation is discussed to give a better understanding of the process.

To compare the thermal performance of TEMs, the established method [7-10], is to plot measures of temperature difference generated across the module (ΔT) versus heat pumped through the module (Q_c) for a given value of current (I) through the device. Q_c is defined in equation 1, where Q_h is the total heat flow through the calorimeter from the hot side of the TEM and P is the electrical power supplied to the module:

$$Q_c = Q_h - P \tag{1}$$

Heat flow through the calorimeter, presented in equation 2, is determined using a best approximation least squares regression fit based on thermistor temperature and spatial positioning, (dT_t/dx) and multiplying by the thermal conductivity (K) and surface area (A) of the copper calorimeter:

$$Q_h = KA\frac{dT_t}{dx} \tag{2}$$

Electrical power delivered to the module is measured as the product of TEM voltage (V) times TEM current (I) and is seen in equation 3:

$$P = VI \tag{3}$$

Temperature difference across the module, seen in equation 4, is the calculation of difference between the constant temperature maintained at the hot side of the module and the temperature measured by the IR sensor on the cold side of the module:

$$\Delta T = T_h - T_c \tag{4}$$

The hot side temperature of the TEM is again determined using a best approximation least squares regression fit similar to Q_h, which is in turn used to calculate the temperature intercept at the surface of the calorimeter [12]. This is computed in real time during the test using Labview software. The cold side temperature is a direct measurement taken by the IR sensor over a spot size of 1mm^2 at the centre of the upper TEM surface.

An uncertainty analysis was also employed in order to quantify the uncertainties associated with each primary measurement and its effect on the calculated properties in the TEM performance characteristics. Each measured quantity and its uncertainty are listed in table 1.

Table 1. Uncertainty in measured quantities

Measured Quantities	**Uncertainty**
Thermistor temperature (T_t)	±0.005°C
Thermistor location (x)	±50μm
Calorimeter area (A)	±1.2825x10^{-6}m^2
Calorimeter thermal conductivity (K)	±5% (W/m K)
IR sensor temperature (T_c)	±0.5°C
TEM Current (I)	±0.01A for 0.3A-3A
TEM Voltage (V)	±1x10^{-4}V for 1V-3V

Many of the measured quantities listed in table 1 were subjected to calibration, and various other steps in order to minimise uncertainty.

- The thermistors used were calibrated, while connected through the vacuum fittings, in the Lauda E100 water bath using a Fluke 1504 reference thermistor, for a temperature range of 15 — 40°C.
- The location of each thermistor along the length of the calorimeter was found using a digital microscope for an optical measurement, which determined the thermistor position to a resolution of 50μm. The area of the calorimeter surface was found in a similar manner.
- Goodfellow supplied the copper used in the calorimeter with an uncertainty of ±5% in the material's thermal conductivity. This value is the largest contributor to uncertainty in heat flow measurements. The author intends to independently characterise the material for further work.
- The cold side temperature measurement is a non-contact IR measurement which was rigorously calibrated in-situ under replicated test conditions. For each increase in heater power setting, the increase in reflected radiation is accounted for in the temperature measurement of the sensor. This was achieved using a copper meter bar with its surface painted with a 20μm layer of black paint, consistent with test TEM, with two 1.2mm diameter, 2mm long, Epcos B57550G502F thermistors calibrated for a temperature range of -30˚C to 30˚C to a certified accuracy of 0.05˚C, embedded 2mm from the surface. The temperature read by the IR sensor was compared to the actual reading of the thermistors in the meter bar, for a range of emissivity values. The temperature range was established on the surface of the meter bar using the secondary TEM to raise and lower temperature. Limiting the accuracy of the IR sensor is the ±0.5˚C repeatability quoted in the device data sheet.
- Current through the test TEM and voltage across it, were measured using certified calibrated meters.

Knowing the accuracy of the measured values, the uncertainties for all calculated values were resolved using the Kline and McClintock method [11] for determining uncertainty in single sample experiments. An example of the maximum uncertainty for each calculated value is displayed in table 2.

Table 2. Maximum uncertainties for calculated quantities

Calculated Quantities	**Maximum Uncertainty**
Power (P)	±1.25%
Heat flow from hot side (Q_h)	±5%
Heat flow from cold side (Q_c)	±5.15%
Hot side temperature (T_h)	±0.25°C
Temperature difference (ΔT)	±0.56°C

This section has discussed the calculated and measured quantities associated with the thermal performance characterisation of TEMs. The uncertainty of measured and calculated quantities were also discussed with uncertainty values given for the relevant measurements in the experimental testing. The data collected is presented and discussed in section 4.

4. Results and discussion

The following results were obtained using the Multicomp MCPF-031-10-25 TEM in a working vacuum of 400Pa. Results are presented and discussed in terms of heat removed from the cold side of the TEM, the temperature difference across it and electrical current through the module. The data is discussed in three subsections for purposes of clarity, beginning with the overall TEM performance characteristics. The special cases of maximum TEM performance, heat pumping from the cold side and temperature difference, are then discussed.

4.1 TEM performance characteristics

Determining the performance characteristics of the test TEM is the primary objective of this study. Figure 2 plots the experimental results of performance in terms of temperature difference as a function of cold side heat pumping for the TEM current range of 0.4A – 2.0A. Included on the plot are the manufacturer's performance curves for the same TEM current to provide a direct comparison. Error bars for cold side heat pumping and temperature difference illustrate the relative uncertainty associated with both measurements.

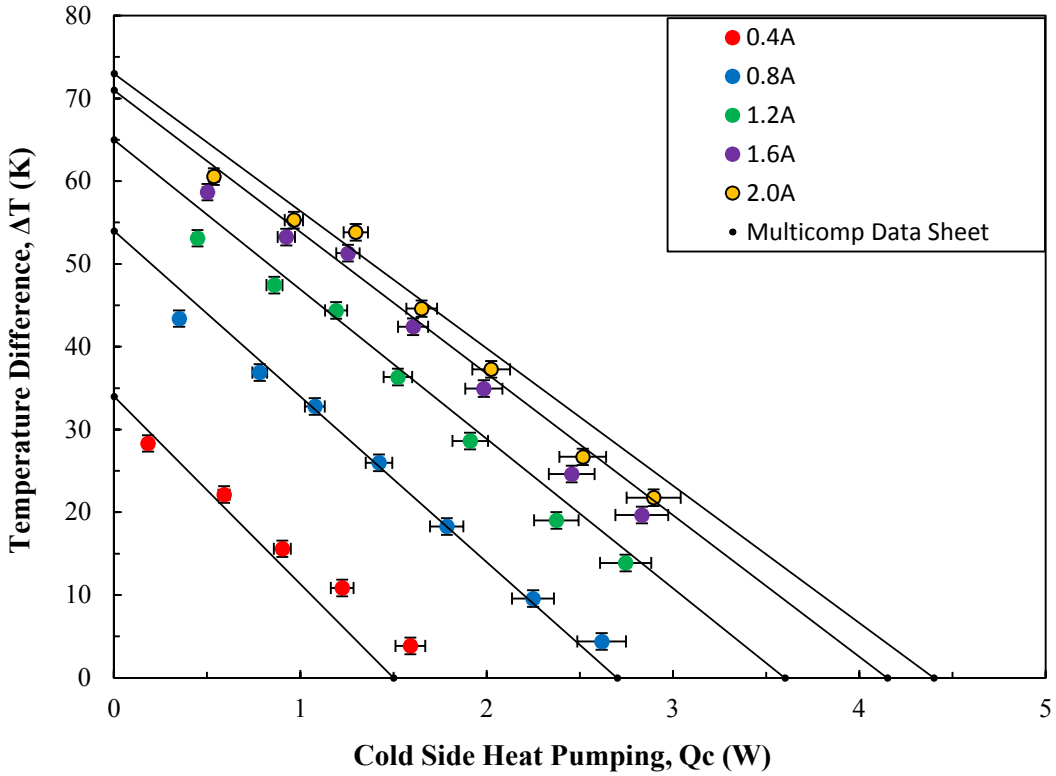

Figure 2. Temperature difference as a function of cold side heat pumping and TEM current, measured data and manufacturer's characteristic curves

Initial impressions from figure 2 confirm the experimental data displayed takes the characteristic linear form expected for thermoelectric performance characteristics seen in [7-10]. There is good agreement between experimental and quoted characteristic behaviour, with slight discrepancies at the highest and lowest current values. Higher current values, 1.6A and 2.0A, show good agreement at higher temperature difference but the data trends towards an under-prediction of cold side heat pumping at lower temperature differences, when compared to the manufacturer's characteristic curves. The differences in trends, especially at lower and higher currents, can be attributed to a fundamental difference in the characterisation method used by the manufacturer. The AC four terminal method, used by Multicomp, is a material level characterisation using electrical measurements to characterise the bulk thermoelectric material which does not fully account for the thermal contribution of the ceramic substrates sandwiching the thermoelectric material and the electrical connections between the thermoelectric pairs in the module. The overall data fit, however, is considered within the expected range.

Areas of particular interest in figure 2 are the cases of maximum TEM performance. These occur at the intersection of the data with the x and y axes, with maximum temperature difference at the y intercept where heat pumping is zero and maximum cold side heat pumping at the x intercept where

temperature difference is zero. For the latter case, only the data sets of lower current values 0.4A and 0.8A cross the x-axis. This is due to the IR heater power limit of 125W, with insufficient heat being supplied to increase the temperature of the upper TEM surface at higher currents. Higher heater power would enable values for temperature difference to approach zero, however this is beyond the range required for the overall objective of the work to characterise μTEMs which have lower heat pumping capabilities and lower temperature differences. It is deemed appropriate for validation purposes to extrapolate a best fit trend line from the data for the x-axis intercept. For the case of maximum temperature difference, the data set, again, does not cross the y-axis. This is due to contributions of radiation heat transfer from surroundings within the evacuated bell jar to the surface of the TEM providing heat for the cold side to pump. It is difficult in this configuration to completely eliminate heat flow from the cold side so an extrapolation of a best fit trend line is necessary to establish the y-axis intercept and maximum temperature difference. These cases of maximum performance are presented in the following sub-sections.

4.2 Maximum heat pumping from TEM cold side

The case of maximum heat pumping from the cold side occurs when the temperature difference across the TEM is zero. As explained in subsection 4.1, the data presented in figure 3 is derived from extrapolated least squares fits of each current setting to the point of the x-axis intercept. Figure 3 plots cold side heat pumping of the test TEM at zero temperature difference across the module, for the current range of 0.4A – 2.0A. Again, experimental and manufacturer's data are compared.

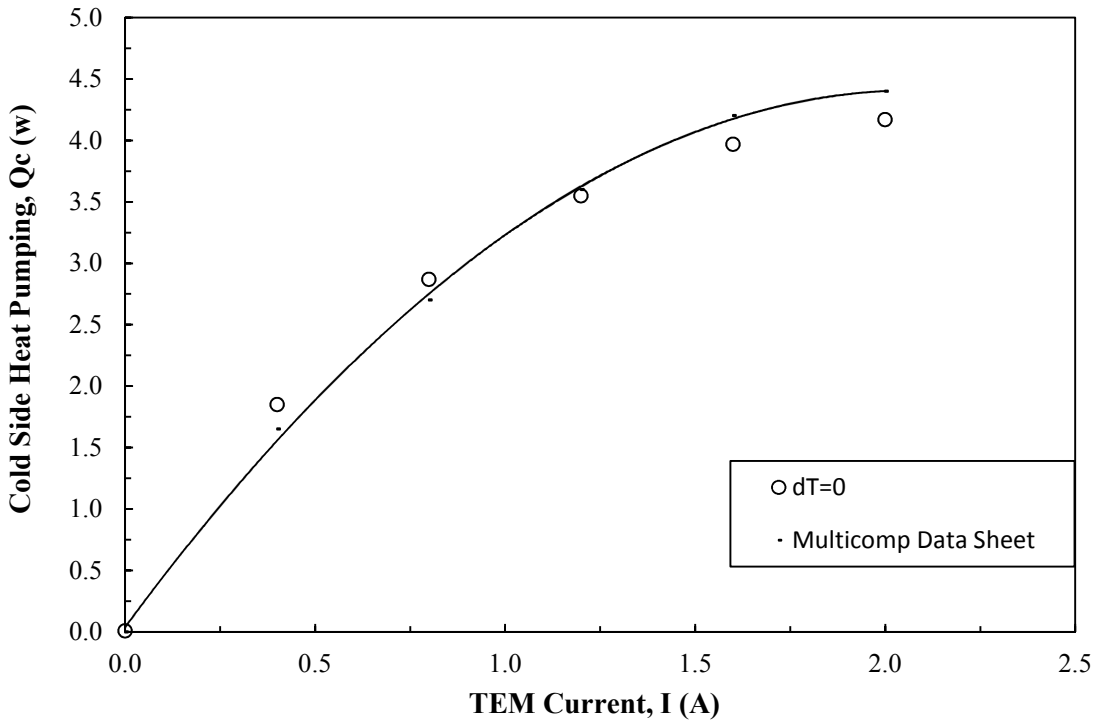

Figure 3. Heat pumped from cold side of TEM as a function of current for the zero temperature difference across module case

Direct comparison of experimental and manufacturer's data for maximum cold side heat pumping for TEM current shows good overall alignment. Slight differences are evident, however, at lowest and highest current values, with the result of marginal difference in trends among measured and quoted data. This is most likely accounted for by the difference in characterisation methods mentioned previously, which is undesirable in a benchmarking process. Despite this, there is good agreement between experimental and quoted data for the current range of 0.4A – 1.2A, with a slightly higher

calculation of heat pumping seen for 0.4A of 0.2W. Lower values of heat pumping at the higher values of current 1.6A and 2.0A, both amount to a difference of 0.23W from manufacturer's quoted data. This represents a 5.2% discrepancy at the maximum heat pumping value at 2.0A, falling marginally outside maximum uncertainty for cold side heat pumping established in section 3. This reflects the expected thermal losses associated with interfacing materials in the TEM, which are approximated in the method used by the manufacturer.

4.3 Maximum temperature difference across TEM

The case of maximum temperature difference across the TEM occurs when heat pumping from the cold side is zero. As explained in subsection 4.1, the data presented in figure 4 is derived from extrapolated least squares fits of each current setting to the point of the y-axis intercept. Figure 4 plots temperature difference across the test TEM versus the current through the module for the condition of zero heat flow through the module. This case represents the maximum temperature difference achievable for each given current value, which is of importance in optical telecommunications applications where the control temperature required can be significantly below the allowable sink temperature. Manufacturer's quoted data is compared to the experimental data.

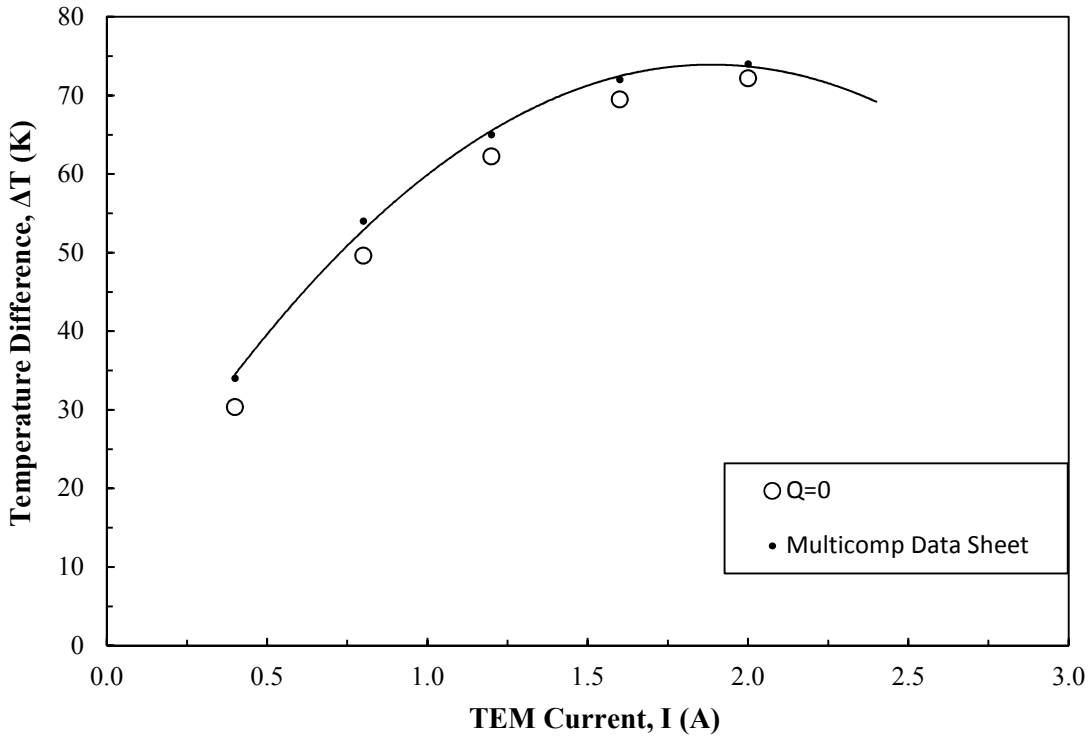

Figure 4. Temperature difference across TEM as a function of current for the zero cold side heat pumping case

Experimental data for temperature difference compare very well with quoted values by the manufacturer. All experimental data points fall less than 3°C from the manufacturer's data series, with that value decreasing for increasing current values. Maximum temperature difference measured at 2.0A by the contactless apparatus falls within 0.9°C of that claimed by the manufacturer. Considering that the Multicomp characterisation method measure temperature difference across the bulk material this is an encouraging outcome that, again, gives confidence in the experimental apparatus and method. Having detailed and discussed the experimental results, the conclusions drawn and further work will be presented.

5. Conclusions

In this paper, a novel contactless method for the characterisation of thermoelectric modules (TEMs) is presented. The method was benchmarked using a commercially available TEM of dimensions 15 x 15 x 4.8mm. Measured data from the experimental apparatus is compared to manufacturer's data sheets, with a view to proving the merit of the novel concept in order to implement the method in a characterisation study of commercially available μTEMs. The following conclusions apply:

- Overall data comparison with manufacturer performance curves yields good agreement, with slight discrepancies evident due to difference in characterisation method.
- The novel contactless characterisation method yields maximum heat pumping from the cold side of the TEM within 5.2% of the manufacturer's quoted data and maximum temperature difference across the TEM within 0.9°C.
- Maximum uncertainty associated with Q_c and ΔT, was calculated at ±5.15% and ±0.27°C respectively.

A contactless method for the characterisation of thermoelectrics was benchmarked successfully allowing further work on μTEMs to proceed with confidence. Future work will include minor adaptations of the apparatus for the measurement of μTEM array performance as well as efforts to further minimise uncertainty associated with primary and calculated measurements, including the characterisation of oxygen free copper to reduce uncertainty in its thermal conductivity.

Acknowledgements

The Author would like to thank Bell Labs, Irish Research Council (IRC) and Science Foundation Ireland (SFI). Bell Labs would like to thank the Industrial Development Agency (IDA) Ireland for their continued support.

References

[1] J. de Boor and V. Schmidt, "Complete Characterization of Thermoelectric Materials by a Combined van der Pauw Approach", *Advanced Materials* **38**, 4303-4307 (2010).
[2] D. Mitrani et al., "Methodology for extracting thermoelectric module parameters", *IEEE Tranactions on Insrumentation and Measurement* 54, 1548, (2005).
[3] T. C. Harman, "Special techniques for measurement of thermoelectric properties", *Journal of Appied Physics* **29**, 1373 (1958).
[4] E. Sandoz-Rosado and R. J. Stevens, "Experimental characterization of thermoelectric modules and comparison with theoretical models for power generation", *Journal of Electronic Materials* 38, 1239 (2009).
[5] S. Dalola et al., "Characterization of thermoelectric modules for powering autonomous sensors", *IEEE Transactions on Instrumentation and Measurement* 58, 99 (2009).
[6] J. D'Angelo and T. Hogan, "Long term thermoelectric module testing system", *Review of Scientific Instruments* **80**, 105102 (2009).
[7] Z. S. Wang et al, "A practical method for measuring thermal conductance and cooling power of thermoelectric modules", in Proc. 20th Int. Conf. on Thermoelectrics, ICT2001, Beijing, China, pp. 515-519, (2001).
[8] R. Ahıska and K. Ahıska, "New method for investigation of parameters of real thermoelectric modules", *Energy Conversion Management* **51**, 338 (2010).
[9] R. J. Buist, "Methodology for testing thermoelectric materials and devices," in CRC Handbook of Thermoelectrics, ed. D. M. Rowe, Boca Raton, FL: CRC Press, ch. 18, (1995).
[10] A. D. Kraus and A. B. Bar-Cohen, Thermal Analysis and Control of Electronic Equipment, McGraw-Hill, ch. 18, (1983)
[11] S. J. Kline & F.A. McClintock, "Describing Uncertainties in Single Sample Experiments" *Mechanical Engineering* **75**, pp. 3-8, (1953)
[12] R. Kempers et al, "A high-precision apparatus for the characterization of thermal interface materials", in Review of Sceintific Instruments **80,** 095111, pp. 1-11, (2009)